ELECTRONIC SUPPLEMENTARY INFORMATION

Composition-Dependent Reactivity of $Ba_{0.5}Sr_{0.5}Co_xFe_{1-x}O_{3-\delta}$ Towards the Oxygen Reduction Reaction

Verónica Celorrio, Devendra Tiwari. David J. Fermín[*]

School of Chemistry, University of Bristol, Cantocks Close, Bristol BS8 1TS, UK.

Table S1. Atomic composition of the various $Ba_{0.5}Sr_{0.5}Co_xFe_{1-x}O_{3-\delta}$ samples. The Ba signal is used as reference.

	Composition (% Atomic)			
	Ba	Sr	Co	Fe
$Ba_{0.5}Sr_{0.5}CoO_{3-\delta}$	0.50	0.55±0.15	1.08±0.16	---
$Ba_{0.5}Sr_{0.5}Co_{0.7}Fe_{0.3}O_{3-\delta}$	0.50	0.49±0.03	0.67±0.03	0.27±0.01
$Ba_{0.5}Sr_{0.5}Co_{0.25}Fe_{0.75}O_{3-\delta}$	0.50	0.56±0.01	0.25±0.01	0.75±0.02
$Ba_{0.5}Sr_{0.5}FeO_{3-\delta}$	0.50	0.50±0.06	---	0.92±0.05

Table S2. Metal cation occupancies and discrepancy factors obtained from Rietveld refinement[§] of PXRD data.

Sample	$Ba_{0.5}Sr_{0.5}CoO_{3-\delta}$	$Ba_{0.5}Sr_{0.5}Co_{0.7}Fe_{0.3}O_{3-\delta}$	$Ba_{0.5}Sr_{0.5}Co_{0.25}Fe_{0.75}O_{3-\delta}$	$Ba_{0.5}Sr_{0.5}FeO_{3-\delta}$
Space group	*Pm-3m*	*Pm-3m*	*Pm-3m*	*Pm-3m*
Ba_{occ}	0.5476(7)	0.5442(6)	0.4711(5)	0.497(7)
Sr_{occ}	0.4524(3)	0.4558(3)	0.5289(6)	0.503(8)
Co_{occ}	1.00	0.7967(7)	0.2161(2)	0.00
Fe_{occ}	0.00	0.2033(6)	0.7839(3)	1.00
$O_{occupancy}$	0.7936(6)	0.8422(5)	0.9045(5)	0.9287(4)
Oxygen content	2.381(2)	2.527(2)	2.714(2)	2.786(1)
Crystallite size (nm)	46	21	23	36
R_{wp} (%)	7.557	7.213	7.233	8.572
R_p (%)	4.326	4.231	4.088	3.971

[§] Quantitative structure refinements were performed on the XRD patterns by the Rietveld method using Fullprof software suite. The analysis starts with calculating a theoretical diffraction pattern from a model structure. To self-consistently adjust the theoretical diffraction pattern to the experimental one, the refinement of the various parameters is performed in the following order: scale factor, specimen displacement, flat background, lattice parameters, further background adjustment, *W* parameter in the Caglioti peak profile function (eq. S1):

$$H = (U \tan 2\theta + V \tan \theta + W)^{1/2} \qquad \text{Eq. S1}$$

atomic coordinates, occupancies and isotropic (thermal) displacement parameters, the parameters *U* and *V* (eq. S1), and other minor profile parameters. Consequently, the XRD line shape is represented using the Cagliotti function, where the parameters *U*, *V*, *W* account for the line shape and width. The quality of fitting is monitored by the statistical correlation coefficients R_p and R_{wp}.

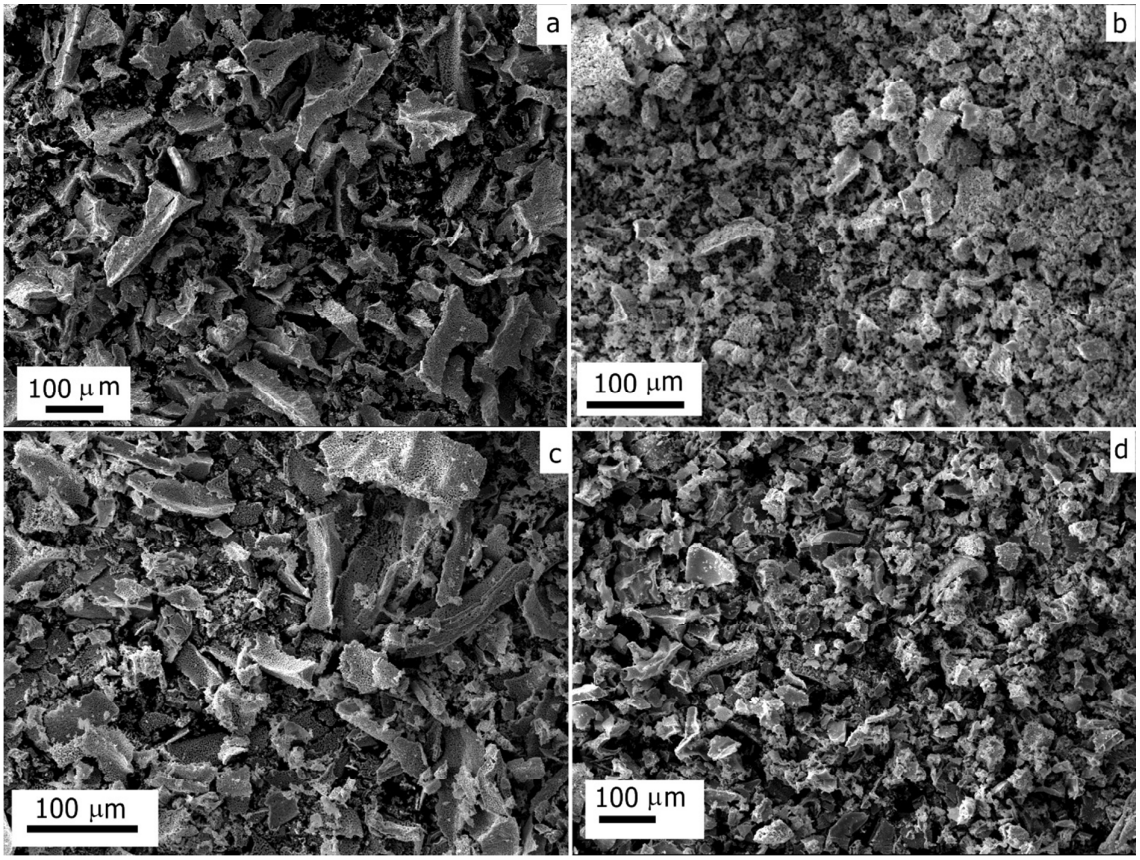

Figure S1. Representative SEM images for $Ba_{0.5}Sr_{0.5}CoO_{3-\delta}$ (a), $Ba_{0.5}Sr_{0.5}Co_{0.25}Fe_{0.75}O_{3-\delta}$ (b), $Ba_{0.5}Sr_{0.5}Co_{0.7}Fe_{0.3}O_{3-\delta}$ (c) and $Ba_{0.5}Sr_{0.5}FeO_{3-\delta}$ (d).

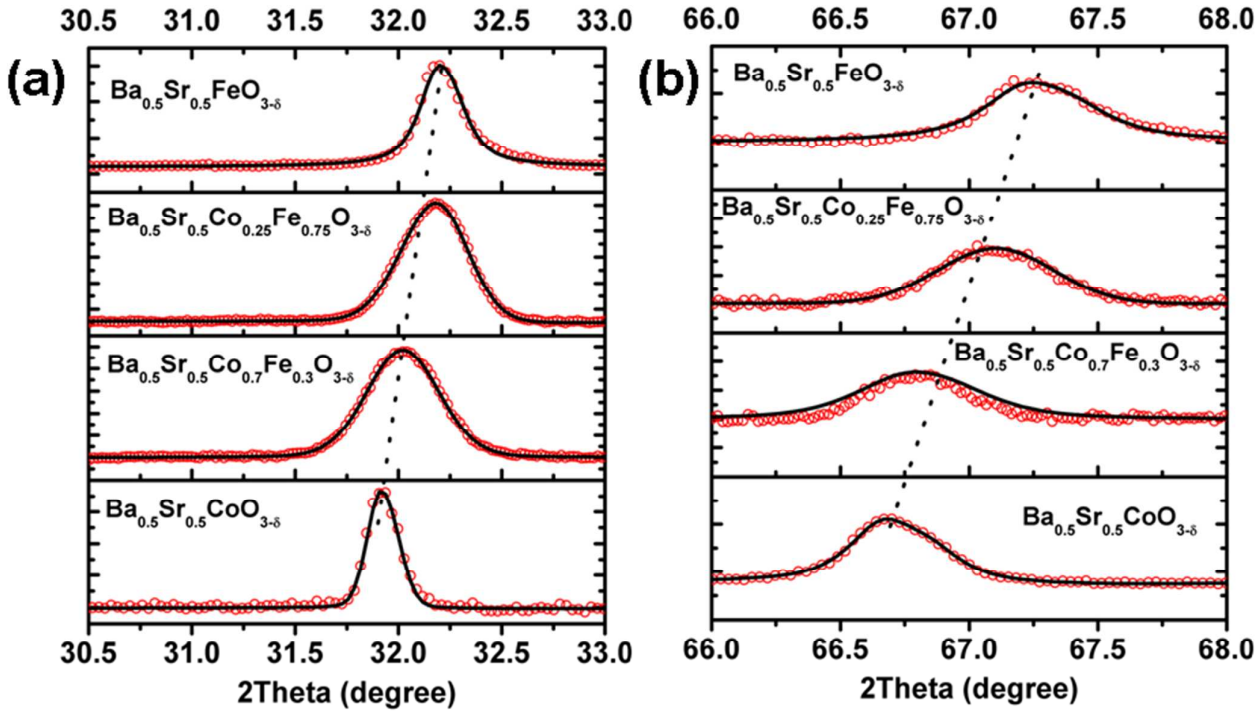

Figure S2. X-ray diffraction patterns for different BSCF compositions in two narrow ranges at (a) 31-33^{o} and (b) 66-68^{o} diffraction angles.

Calculation of HO_2^- yield and the number of electrons (n_e) involved in the reaction calculated using i_R and i_D

The HO_2^- yield can be calculated as from:

$$X_{HO_2^-} = \frac{2i_R/N}{i_D + i_R/N} \times 100 \qquad \text{Eq. S.1}$$

where N is the collection efficiency of the rotating-ring disc electrode (determined to be 0.42 by employing ferrocene methanol as the redox probe). The effective number of electrons involved (n_e) in the ORR can be estimated from:

$$n_e = 4 \cdot \frac{i_D}{i_D + i_R/N} \qquad \text{Eq. S.2}$$

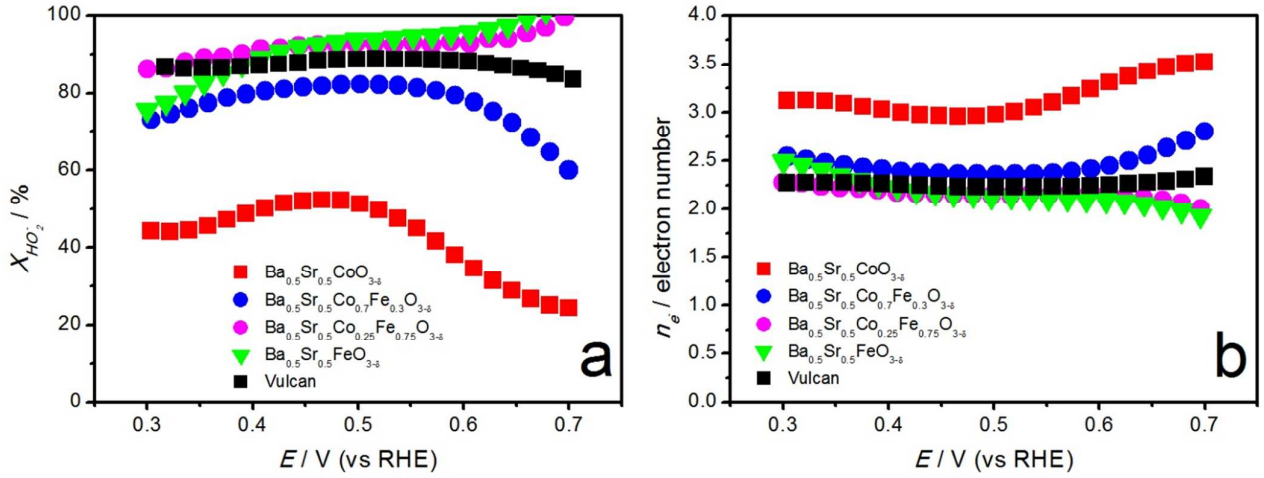

Figure S3. Yield of HO_2^- formation (a) and effective number of electrons (b) transferred during ORR.

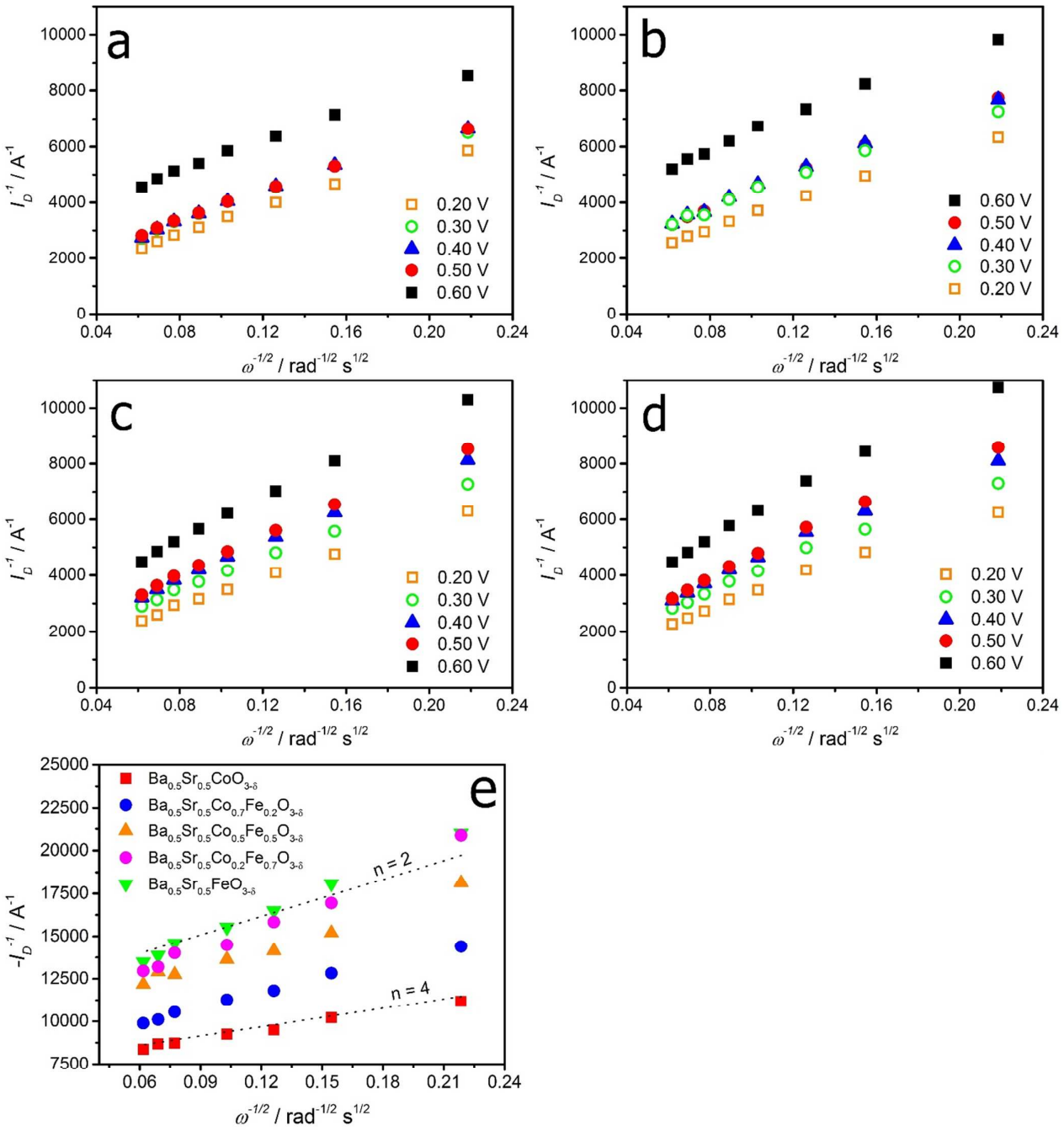

Figure S4. Koutecky-Levich at various potentials for $Ba_{0.5}Sr_{0.5}CoO_{3-\delta}$ (a), $Ba_{0.5}Sr_{0.5}Co_{0.7}Fe_{0.3}O_{3-\delta}$ (b), $Ba_{0.5}Sr_{0.5}Co_{0.25}Fe_{0.75}O_{3-\delta}$ (c) and $Ba_{0.5}Sr_{0.5}FeO_{3-\delta}$ (d) electrodes in O_2-saturated 0.1 M KOH solution at different potentials. Figure (e) shows the Koutecky-Levich plot for the various $Ba_{0.5}Sr_{0.5}Co_xFe_{1-x}O_{3-\delta}$ composite electrodes in O_2-saturated 0.1 M KOH solution at 0.65 V. Dotted lines represent the theoretical values for the 2 and 4-electron pathways.

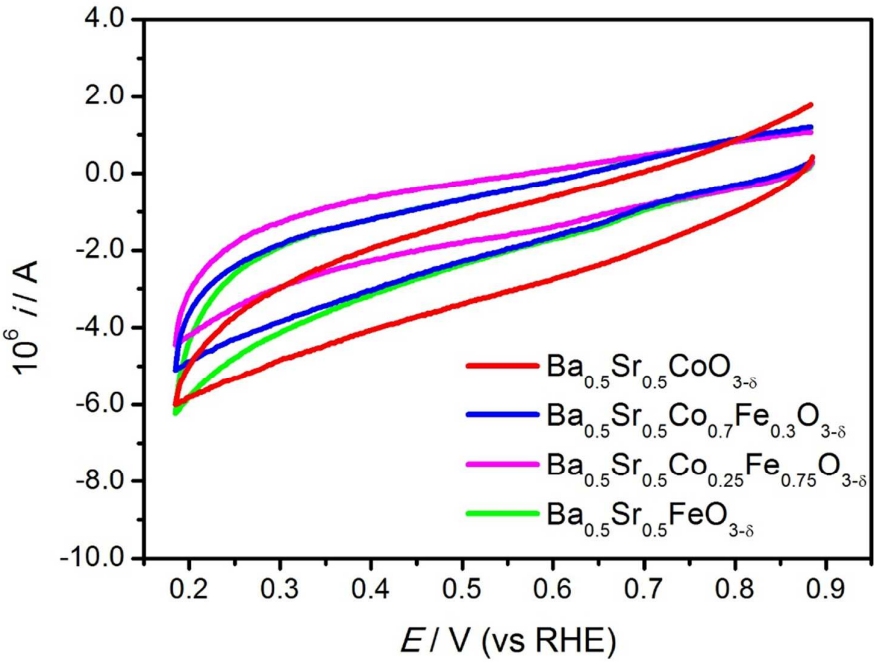

Figure S5. Cyclic voltammograms of the Vulcan supported oxides in Ar purged 0.1 M KOH solution at 10 mV s^{-1}. Oxide loading is identical to those reported in figure 3. The lack of electrochemical responses arising from changes in the oxidation state of the B-site strongly suggest that the material is highly stable within this potential range.